RSC Advances

PAPER

View Article Online
View Journal | View Issue

Cite this: *RSC Adv.*, 2025, **15**, 23670

Profiling characteristics of plasma exosomal miRNAs across cognitive stages: from normalcy to mild cognitive impairment and Alzheimer's disease†

Xi Chen,‡[a] Silu Chen,‡[a] Liangliang Chen,‡[a] Hong Zheng,[a] Jing Nie,[b] Lingyan Yang,*[c] Xia Li*[b] and Kang Ju *[a]

The rising global prevalence of Alzheimer's disease (AD) and mild cognitive impairment (MCI) underscores the urgent need to elucidate their underlying pathogenic mechanisms. This study investigated the dynamic alterations of plasma-derived exosomal miRNAs across the cognitive spectrum from normal cognition (NC) through MCI to AD, and their potential pathogenetic implications. Here, we enrolled 10 AD patients, 9 MCI patients, and 10 normal cognitive (NC) patients rigorously diagnosed using amyloid PET imaging, cerebrospinal fluid biomarkers, and standardized neuropsychological assessments. Serum exosomes were isolated and identified, then small RNA sequencing was performed. The results revealed distinct exosomal miRNA expression profiles across disease stages, with 10 conserved miRNAs showing progressive dysregulation along the NC–MCI–AD continuum. Target gene prediction formed numerous miRNA–mRNA pairs. GO and KEGG enrichment indicated that exosomal miRNAs might affect cognitive decline by regulating neurodevelopment and cell senescence. Strikingly, ROC analysis demonstrated superior diagnostic performance for miR-151a-3p and miR-210-3p in distinguishing disease states. Our findings not only characterize stage-specific exosomal miRNA signatures during AD progression but also identify novel circulating biomarkers with diagnostic potential. This work provides mechanistic insights into exosome-mediated pathological processes and advances the development of liquid biopsy approaches for early detection and therapeutic monitoring in neurodegenerative diseases.

Received 29th April 2025
Accepted 28th June 2025

DOI: 10.1039/d5ra02993g

rsc.li/rsc-advances

Introduction

With the acceleration of the aging process in Chinese society, the prevalence of Alzheimer's disease (AD) has been rising significantly. Statistically, there are 15.07 million dementia patients aged 60 years and above in China, of which 9.83 million are AD patients, 3.92 million are vascular, and 1.32 million are patients with other forms of dementia.[1] As one of the most common neurodegenerative diseases in the elderly population, AD is anatomically characterized by neocortical atrophy, neuronal and synaptic loss, and the main pathological features, including extracellular amyloid β-protein (Aβ) deposition plaques and intracellular neurofibrillary tangles (NFTs).[2,3] Due to the long-term and latent nature of the pathological progression of AD, its clinical presentation can be categorized as cognitively normal, mild cognitive impairment (MCI), and full-blown AD.[4] MCI is a transitional state between normal cognitive aging and symptomatic AD, characterized by a degree of memory loss that is not age-appropriate, but has not yet met the clinical diagnostic criteria for dementia.[5] Longitudinal cohort studies have shown that neuropathologic changes such as Aβ deposition begin to slowly progress in the early stages of MCI.[6] Despite the progress made in studying AD and MCI, their pathogenesis and progression are still not fully understood. Early diagnosis of AD and MCI is crucial in current clinical practice and research.

Exosomes, as a circular structure delimited by a lipid bilayer (30 to 150 nm in diameter), can carry a variety of nucleic acids such as DNA, mRNA, miRNA, *etc.*, protecting their contents from degradation.[7–9] Exosomes can be released from serum, neurons, astrocytes, oligodendrocytes, and microglia and play a key role in synaptic communication, nerve regeneration, and degeneration.[10–12] Considering the stability and wide distribution of exosomes, the miRNAs they carry are highly susceptible to the disease microenvironment, and their expression may be altered in different diseases and processes.[13,14] This expression

[a]*Shanghai Changning Mental Health Center, Affiliated Mental Health Center of East China Normal University, Xie He Road 299, Shanghai 200335, China. E-mail: allston@163.com; chensilu0724@163.com; chenll2006@126.com; zhhmm2@163.com; kangjuencuamhc@163.com*

[b]*Shang Hai Jiao Tong University, Shanghai Mental Health Center, Wan Ping Road 600, Shanghai 200030, China. E-mail: niejing@alumni.sjtu.edu.cn; lixia11111@sjtu.edu.cn*

[c]*Guangzhou National Laboratory, No. 9 Xing Dao Huan Bei Road, Guangzhou International Bio Island, Guangzhou 510005, China. E-mail: yang_lingyan@gzlab.ac.cn*

† Electronic supplementary information (ESI) available. See DOI: https://doi.org/10.1039/d5ra02993g

‡ These authors contributed equally.

fluctuation, which is tightly coupled with the disease process, has made exosomes a hotspot for the study of potential biomarkers for a variety of diseases, especially in AD.[15] Recently, serum exosomes and their miRNAs have attracted much attention in the field of neurodegenerative diseases, and have shown great potential as new targets for disease diagnosis and treatment due to their specific changes in disease development.[16] Increasingly, studies have been conducted to detect a variety of potential, utilizing biomarkers for neurodegenerative diseases in blood, plasma, and serum, and employing small RNA sequencing technolog. Previous studies have demonstrated significant differences between AD patients and healthy populations in the assessment of cognitive function. For example, the combination of miR-30b-5p, miR-22-3p, and miR-378a-3p, and the combination of miR-135a, miR-193b, and miR-384 were found to be significantly dysregulated in AD, which can be used for the early diagnosis.[17,18] However, the molecular mechanisms underlying the progression of NC to MCI and then to AD, especially the pattern of exosomal miRNA expression and related molecular pathways, still need to be further explored.

In this study, the comparative analysis of MCI, AD patients, and the NC group was used to clarify the differences in baseline data, especially the characteristics of cognitive function. Through a series of experiments, the molecular mechanisms involved in the progression from a healthy state to MCI or even AD, especially the role of exosomal miRNAs, will be investigated in depth. This study is expected to provide more valuable biomarkers for the early diagnosis of AD and MCI, as well as a theoretical basis for the development of effective therapeutic strategies for disease progression.

Materials and methods

Participants and clinical data

Clinical blood samples were obtained from patients from January 2022 to August 2024 at the Shanghai Mental Health Center and Changning District Mental Health Center in China. According to the diagnostic criteria of the International Classification of Diseases, 10 patients with Alzheimer's disease (AD), 9 patients with mild cognitive impairment (MCI), and 10 individuals with normal cognitive function (NC group) were included. All participants were assessed by the Mini-Mental State Examination (MMSE), the Montreal Cognitive Assessment Scale (MOCA), and the Clinical Dementia Rating (CDR). The study was approved by the Ethics Committee of the Shanghai Mental Health Center (Grant No. SHMEC-2021-008), and written informed consent was signed by patients or legal guardians.

Inclusion and exclusion criteria are described below. AD patients were diagnosed based on the 2018 National Institute on Aging Alzheimer's Association (NIA-AA) Core Clinical Criteria and combined with the criteria of reduced CSF Aβ42 and positive amyloid-PET.[5,19,20] Participants were aged 55–85 years with primary education or higher, Geriatric Depression Scale (GDS) total score ≤ 10, CDR > 0.5 and ≤ 2, and Harkinsky Ischemia score < 4. All AD patients had completed cranial MRI to exclude significant structural brain abnormalities.

Patients with MCI met the 2011 NIA-AA diagnostic criteria for mild cognitive decline and met the criteria for reduced cerebrospinal fluid Aβ42 levels and amyloid PET positivity. Participants were aged 55–80 years with primary education or higher, GDS total score ≤ 10, CDR $= 0.5$, and Hutchinsky Ischemia Index Scale score < 4. Critical area infarcts and severe white matter lesions were excluded by cranial MRI.

The individuals with normal cognition were recruited with age matching to the case group (± 5 years); MMSE ≥ 26 points; normal visual and auditory function without complaints of cognitive impairment; no abnormalities in physical and neurological examinations. Patients with malignant tumors, uncontrolled severe metabolic diseases, a history of cerebrovascular disease, severe hepatic or renal insufficiency, and other neurological diseases were excluded.

Clinical and cognitive assessment

Cognitive assessments included measures of global cognitive status, the MMSE, and MOCA, along with tests designed to assess more specific cognitive domains.[21] CDR was used for grading the AD by an experienced neuropsychiatrist.[22] At the same time, we also used GDS to eliminate depression that scored higher than ten. All the assessors passed the consistency test.[23]

Blood preparation and exosome isolation

Blood samples were centrifuged at $3000\times g$ for 15 min at 4 °C to separate serum. Exosomes were isolated using the Beckman (Microfuge 20R) Exosome Isolation Kit (Beckman Coulter, USA) according to the manufacturer's instructions. Briefly, serum was centrifuged at $2000\times g$ for 30 min at 4 °C to remove cells and debris, and then at $10\,000\times g$ for 45 min to remove larger vesicles. The supernatant was collected, filtered through a 0.45 μm membrane, and transferred to a new centrifuge tube. The supernatant was removed by centrifugation at $100\,000\times g$ for 70 min at 4 °C and repeated twice. The resulting precipitate was resuspended with 200 μL of pre-cooled 1× PBS, and the exosome concentration was determined by BCA protein quantification, dispensed, and stored at −80 °C. The size and morphological features of exosomes were examined by transmission electron microscopy (TEM, JEM1230). Nanoparticle tracking analysis (NTA, ZetaView) was used to observe the diameter distribution and concentration of exosomes. The surface markers (CD9 and CD81) of exosomes were identified by nano-flow cytometry (NanoFCM, N30E). The exosomal positive protein markers (TSG101, CD9 and CD81) and negative protein marker Calnexin, were confirmed by western blot analysis. The antibodies used were as follows: CD9 (Cat. No. A1703, Abclonal), CD81 (Cat. No. 41779, SAB), Calnexin (Cat. No. ab22595, Abcam), and TSG101 (Cat. No. ab133586, Abcam).

RNA extraction

The total RNA of serum exosomes was extracted by the TRIzol method. Briefly, the exosome suspension was added with chloroform, shaken and then left at room temperature, followed by centrifugation at $12\,000\times g$ at 4 °C. The upper layer was

transferred to a new tube with isopropanol and centrifuged at 4 °C. The supernatant was removed, the precipitate was washed with 75% ethanol, and DEPC water was added to dissolve the RNA. The concentration and integrity of the obtained RNA were determined on a NanoDrop 2000 (Thermo Scientific, USA), agarose gel electrophoresis, and Agilent 2100 Bioanalyzer (Agilent Technologies, USA).

Small RNA sequencing

The small RNA libraries were constructed using the NEB Next Multiplex Small RNA Library Prep Set for Illumina (New England Biolabs Inc, USA) according to the manufacturer's instructions. Briefly, 3′ and 5′ adapters were ligated using ligase, double-stranded cDNA was synthesized by reverse transcription of RNA using superscript II reverse transcriptase, and PCR was performed to amplify the enriched DNA fragments. The target fragment size products were separated by 15% PAGE gel, and the miRNA library was finally obtained. Quality control was performed on the library, followed by PE150 sequencing on the Illumina HiSeq 2500 platform. Subsequently, the raw data were quality assessed using fastp, and trimmomatic was used to remove low-quality bases and adapter sequences to obtain high-quality clean read. The clean reads were aligned with the miRBase database using miRDeep2 to identify known miRNA. Meanwhile, novel miRNAs were predicted by mireap (v0.2) based on their secondary structure, expression and other features. The miRNA expressions among different groups were statistically analyzed using DESeq v1.39.0, and the conserved miRNAs with significant differences were classified according to $|\log2foldchange| > 1$ and P-value < 0.05. The target gene prediction was performed by miRanda v3.3a using the 3′ UTR of the mRNAs as the target sequence for the differentially expressed miRNA sequence. To explore the biological processes and signaling pathways involved in the differential miRNAs, Gene Ontology (GO) functional enrichment of the target genes was performed using topGO v2.50.0, and Kyoto Encyclopedia of Genes and Genomes (KEGG) pathway analysis of the target genes was conducted using clusterProfiler (4.6.0) software.

Statistical analysis

Clinical data were processed by SPSS 25.0 statistical software (IBM Corp. Armonk). Data following normal distribution were analyzed by one-way analysis of variance (ANOVA) for group comparisons, and significant differences were determined by Tukey's HSD test. Comparisons of differences between groups for non-normal distribution data were performed by the Kruskal–Wallis H-test, and significant differences were analyzed by the Mann–Whitney U-test. $P < 0.05$ indicated statistical significance. The predictive accuracy of miRNAs was evaluated by s receiver operating characteristic (ROC) analysis. ROC curves were constructed using different disease processes as state variables and miRNA expression levels as test variables. The area under the curve (AUC) was calculated to evaluate the efficacy of each miRNA for disease diagnosis or distinguishing different disease stages. The closer the AUC value was to 1, the higher the diagnostic accuracy was.

Results

Baseline data

Baseline characteristics for the AD ($n = 10$), MCI ($n = 9$), and NC groups ($n = 10$) are displayed in Table 1. The results showed that there were no significant differences among the three groups in terms of age, gender distribution, and years of education. However, there were significant differences among the three groups in the assessment of cognitive functioning. The MMSE and MOCA scores were significantly lower in the AD group than in the MCI and NC groups, whereas there were no significant differences between the MCI and NC groups. In terms of CDR scores, there were significant differences between the AD group and the MCI and NC groups, as well as between the MCI and NC groups. Overall, cognitive function was significantly impaired in the AD and MCI groups compared to the NC group, and the degree of cognitive impairment was more severe in the AD group than in the MCI group.

Characterization of circulating exosomes

Serum exosomes were identified by TEM and NTA, and the TEM results visualized the typical cup-shaped morphology of exosomes with a clear membrane structure, which was consistent with the characteristics of exosomes (Fig. 1A). NTA analysis showed that the diameter of exosomes ranged from 68 to 155 nm, which was within the common particle size range, and the average particle size distribution was 92.4 ± 24.1 nm (Fig. 1B). Further, CD9 and CD81, two common markers on the exosome surface, were detected by nanoflow technology. Fluorescently labeled anti-CD9 and anti-CD81 antibodies specifically bound to exosomal surface antigens, and the fluorescence signals were analyzed by flow cytometry. The results showed that both CD9 and CD81 were positively expressed in the exosome samples, with a positive rate of 8.4% and 5.6%, further confirming that the extracted vesicles were exosomes (Fig. 1C). We further confirmed the exosomal content by western blot analysis, the results showed CD9 and CD81, and also TSG101, which is a common internal protein marker of the exosome, were enriched on the exosomes. Meanwhile, the Calnexin, the endoplasmic reticulum marker, was negative detected (Fig. 1D). Together, these results indicated that we isolated purity exosomes from serum with ultracentrifugation.

Changes in serum exosomal miRNA expression profiles from NC to MCI and then to AD

To explore the molecular mechanisms in the development of a healthy state to MCI or even AD, especially the role of miRNA, miRNA sequencing analysis was performed on the serum exosomes of each group. The raw reads for each sample ranged from 11 485 623 to 32 768 945 (ESI Table 1†). After quality control, the remaining number of reads per sample ranged from 3 689 023 to 28 971 546. These high-quality reads were then mapped to the miRBase database. The total number of mature miRNAs expressed in each sample ranged from 280 to 386. Regarding sequence annotation, the number of annotated piRNAs ranged from 2113 to 20 063; rRNAs from 788 to 69 918;

Table 1 Summary of clinical information for the AD, MCI and NC groups[a]

Characteristics	AD ($n = 10$)	MCI ($n = 9$)	NC ($n = 10$)
Age (years)	67.3 ± 8.77[a]	70.1 ± 11.17[a]	67.56 ± 2.13[a]
Gender (male/female, *N*)	2/8, 10[a]	2/8, 10[a]	1/7, 9[a]
Education (years)	10.05 ± 2.12[a]	8.9 ± 1.97[a]	9.44 ± 1.81[a]
Mini-mental state examination (MMSE)	7.50 ± 3.21[b]	22.1 ± 3.70[a]	26.44 ± 1.73[a]
Montreal cognitive assessment scale (MOCA)	8.40 ± 6.65[b]	23.5 ± 3.44[a]	27.46 ± 1.42[a]
Clinical dementia rating (CDR)	2.30 ± 0.67[a]	0.54 ± 0.08[b]	0.36 ± 0.18[b]

[a] Data are presented as mean ± SEM, and different letters in the upper right corner indicate statistically significant differences among groups (Kruskal–Wallis H-test, $P < 0.05$).

tRNAs from 9789 to 3 745 901; snRNAs from 52 to 1580; and snoRNAs from 52 to 7269. Meanwhile, new miRNAs were also identified, with a number of 1–87 per sample. In terms of genome structure mapping, the number of sequences mapped to intron regions ranged from 46 131 to 1 022 261 sequences, and exon regions ranged from 11 831 to 367 805 sequences.

Subsequently, we performed an in-depth analysis of miRNA expression across groups. The miRNA expression profiles of the three groups were observed by principal component analysis and Pearson correlation analysis. The results showed that the samples from NC, MCI, and AD groups presented obvious distributional differences, and the samples within the groups showed some similarity in expression (Fig. 2A and B). Initially, it was shown that the miRNA expression profiles changed significantly from a healthy state to MCI and then to AD. We further compared the specific miRNAs that were differentially expressed among different groups. Comparing the NC and MCI groups, 60 miRNAs were up-regulated and 386 miRNAs were down-regulated (Fig. 2C). In the MCI *versus* AD group, 254 miRNAs were upregulated and 70 miRNAs were downregulated (Fig. 2D). When NC was compared with the AD group, 64 miRNAs were up-regulated and 59 miRNAs were down-regulated (Fig. 2E). Venn diagrams show the overlap of differentially expressed miRNAs within the different comparison groups (Fig. 2F). Notably, 10 miRNAs were differentially expressed in the NC *versus* AD, MCI *versus* AD, and NC *versus* MCI

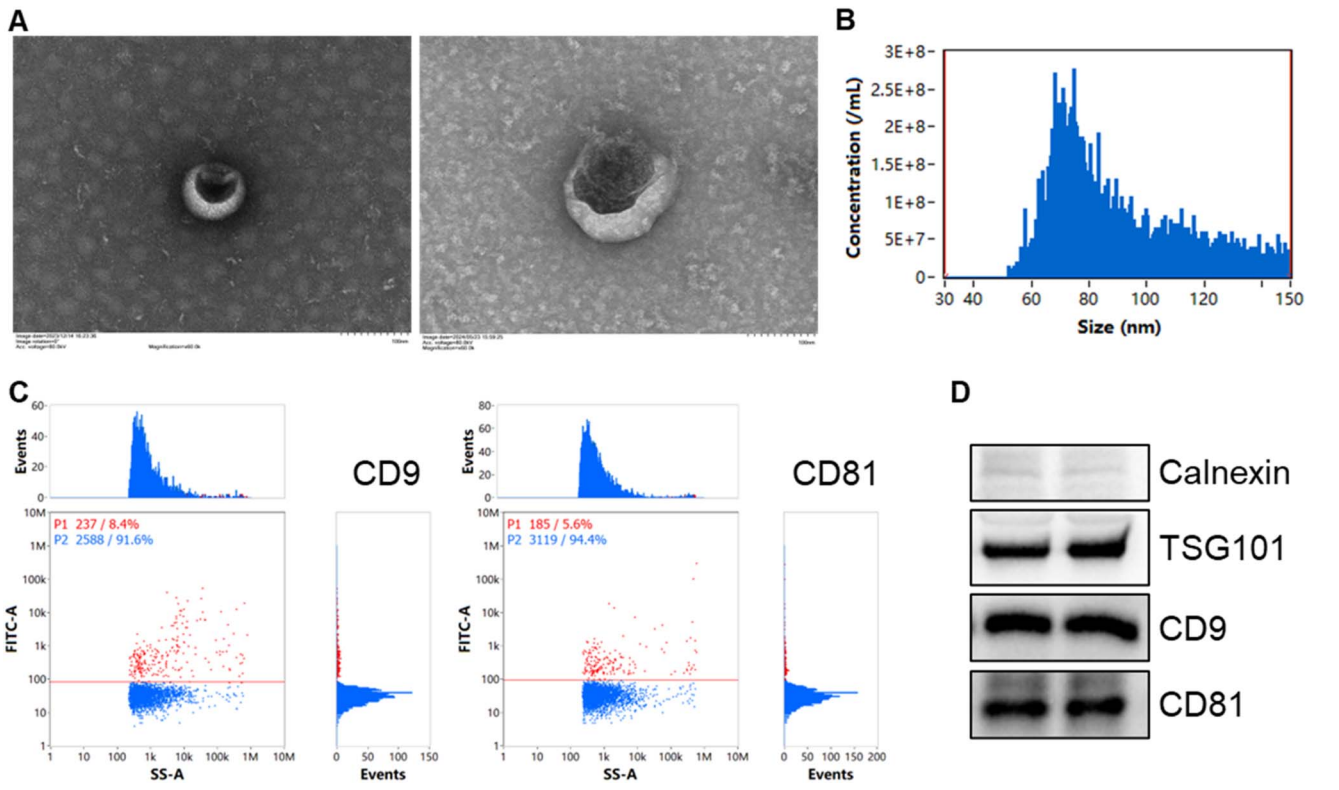

Fig. 1 Serum exosomes isolation and identification. (A) Representative morphological structures of exosomes observed by transmission electron microscopy (scale bar: 100 nm). (B) Particle size distribution analysis of exosomes by nanoparticle tracking analysis. (C) Expression of exosome markers CD9 and CD81 detected by nano-flow analysis. The P1 and P2 regions represent the different cell populations and their proportion, respectively. (D) Western blot analysis of Calnexin, CD9, CD81, and TSG101 detected expression on the exosomes.

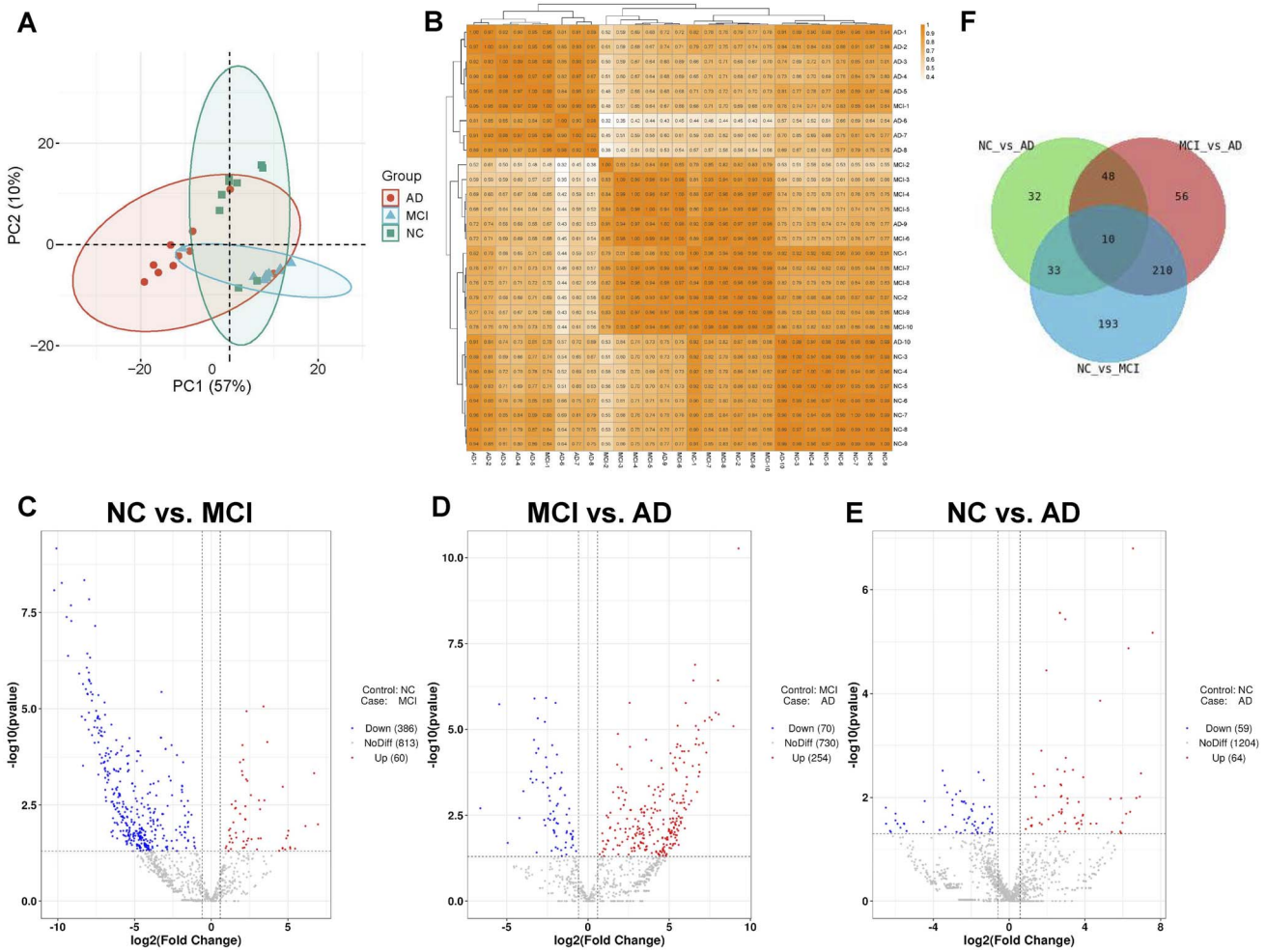

Fig. 2 Changes in serum exosomal miRNA expression profiles of NC progressing to AD. (A) Principal component analysis of the distribution of miRNA expression profiles of samples in each group. (B) Pearson correlation analysis. Color shades represent the strength of correlation. (C–E) Volcano plots demonstrating differentially expressed miRNAs between NC and MCI, MCI and AD, and NC and AD groups. Red dots indicate up-regulated miRNAs, blue dots indicate down-regulated miRNAs, and grey dots indicate miRNAs with no significant difference. (F) Venn plots demonstrating the overlap of differentially expressed miRNAs between different comparative groups. NC, normal control; MCI, mild cognitive impairment; AD, Alzheimer's disease.

comparisons (ESI Table 2†). This suggests that these 10 miRNAs may play a key role in the transition from normal state to MCI and AD, which provides important clues for further exploration of disease-related molecular pathways and potential therapeutic targets.

Functional differences in miRNAs contribute to AD disease progression

We performed target gene prediction of miRNA sequences using Miranda to target the 3′UTR sequences of mRNAs, and further explored the mechanism of exosomal miRNAs in the AD process. In the NC *vs.* MCI group, GO bioprocess enrichment analysis revealed significant enrichment of anatomical structure development, developmental process, and regulation of response to stimulus entries (Fig. 3A). The cellular components were mainly related to organelles, cytoplasm and vesicle, while the molecular functions were related to protein and ion binding. KEGG enrichments showed that axon guidance, neurodegeneration, calcium, hippo signaling pathway, cellular senescence, and AD were significantly enriched (Fig. 3B). For the MCI *vs.* AD group, the entries of the developmental process, cell communication, transport, nervous system development, and nitrogen compound transport were significantly enriched, and the cellular components and molecular functions were similar to those of the NC *vs.* AD group (Fig. 3C). KEGG analysis revealed that neurodegeneration, amyotrophic lateral sclerosis, axon guidance, AD, cellular senescence, fluid shear stress and atherosclerosis were significantly enriched (Fig. 3D). Among the NC *vs.* AD group, GO biological processes were enriched for developmental process, cell communication, response to stimulus, nervous system development, and cellular components were concentrated in intracellular anatomical structure and cell junction (Fig. 3E). In the KEGG pathway, axon guidance, calcium signaling pathway, focal adhesion, chemokinesis, and focal junction were enriched in the developmental process, regulation of cell communication, regulation of response to

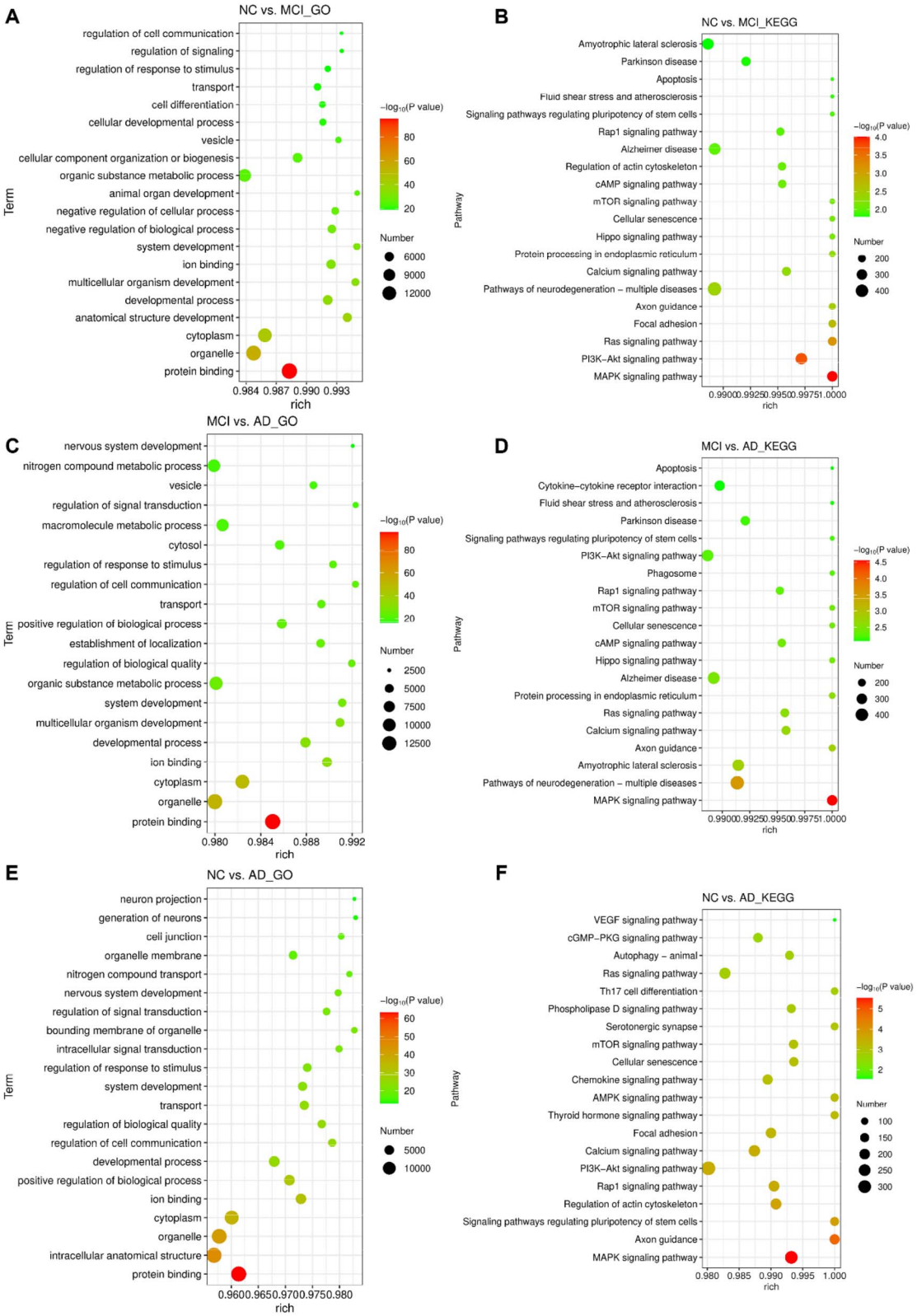

Fig. 3 Functions of differentially expressed miRNA target genes in GO and KEGG analyses. (A and B) Enrichment of NC *vs.* MCI comparison group in GO and KEGG analyses. Enrichment factors are used as horizontal coordinates, bubble color and size represent significance and number of genes enriched, respectively. (C and D) Enrichment results of MCI *vs.* AD comparison group. (E and F) Enrichment results of NC *vs.* AD comparison group.

stimulus, nervous system development, and generation of neurons, *etc.*, and the cellular components were concentrated in the intracellular anatomical structure and cell junction. KEGG signaling pathways such as axon guidance, focal adhesion, calcium, chemokine, and VEGF signaling pathways were significantly enriched (Fig. 3F). Overall, exosomal miRNAs in the progression of NC to MCI and AD may affect cognitive decline by regulating common biological processes and signaling pathways such as neurodevelopment, cellular communication, neurodegeneration and cellular senescence, which collectively contribute to disease progression.

Target genes and function prediction of 10 common miRNA

We further analyzed target gene prediction for 10 key miRNAs commonly identified in the 3 comparative groups, pairing to 11

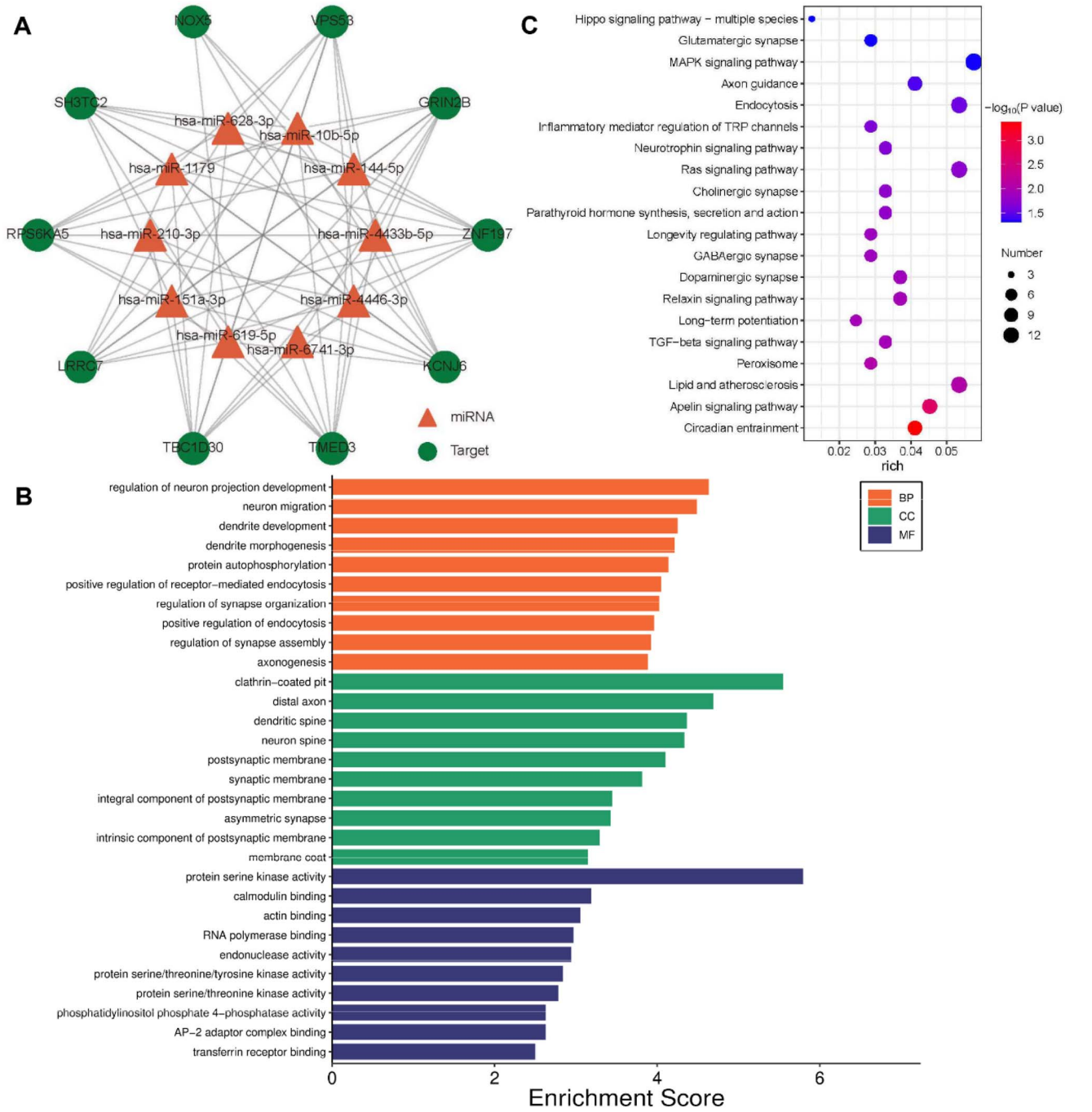

Fig. 4 Target genes and function prediction of 10 common miRNA. (A) Interaction network diagram of miRNAs and their targets. Triangles represent miRNAs and circles represent target mRNAs. Lines represent the interactions between miRNAs and mRNAs. (B) GO enrichment analysis of target genes. BP, biological process; CC, cellular component; MF, molecular function. (C) Scatter plot of enrichment analysis of KEGG pathway for target gene.

813 mRNAs, forming 23 855 miRNA–mRNA pairs. Among them, TBC1D30, KCNJ6 and TMED3 were targeted by 9 miRNAs; ZNF197, VPS53, GRIN2B, NOX5, RPS6KA5, SH3TC2 and LRRC7 were targeted by 8 miRNAs (Fig. 4A and ESI Table 3†). Another 47, 141, and 367 genes were targeted by 7, 6, and 5 miRNAs, respectively. Subsequently, we analyzed the functional enrichment of 565 target genes targeted by 5 or more miRNAs. The results showed that these target genes were significantly enriched in neuron projection development, neuron migration, dendrite development, and axonogenesis (Fig. 4B). They were mainly found in the distal axon, dendritic spine, postsynaptic membrane and other cellular components, and were involved in molecular functions related to protein serine kinase activity, calmodulin binding, actin binding and other molecules. Signaling pathway analysis revealed that they were significantly enriched in the apelin signaling pathway, lipid and atherosclerosis, longevity regulating pathway, axon guidance and hippo signaling pathway (Fig. 4C). These suggested the key role of these miRNAs in biological processes related to nervous system development.

ROC curve analysis of differentially expressed miRNAs

Based on the 10 common differentially expressed miRNAs detected in different comparative groups (NC *vs.* MCI, MCI *vs.* AD, NC *vs.* AD), we extracted their expression data and performed ROC curve analysis (ESI Table 2†). The results showed that several miRNAs exhibited great potential as potential biomarkers for disease diagnosis or progression. For example, miR-151-3p, miR-4433b-5p, miR-628-3p, and miR-210-3p all showed ROC curve area under the curve (AUC) greater than 0.8 among the three groups (Fig. 5A and B). Notably, the AUC values of miR-210-3p and miR-151-3p were higher than 0.9, respectively, showing high sensitivity and specificity, which demonstrated their excellent potential in identifying NC, MCI and AD patients. The AUC values of miR-10b-5p and miR-144-5p reached 0.79, close to 0.8, respectively, showing moderate predictive efficacy. In contrast, the AUC values of miR-619-5p, miR-1179, miR-4446-3p, and miR-6741-3p were lower and had limited predictive ability. Overall, the ROC curves and corresponding AUC values provided a valid basis for evaluating the potential value of different miRNAs as biomarkers to differentiate samples.

Discussion

This study focuses on the plasma-derived exosomes miRNAs in the three stages of the AD spectrum, aiming to deeply analyze the key biological changes during the progression from a normal cognitive state to MCI or even AD, and to provide a strong basis for early diagnosis, intervention and development of therapeutic targets.

Since the expression levels of miRNAs may be affected by various factors,[24–26] we established strict exclusion criteria to equalize the age, gender distribution, and years of education between the MCI, AD, and NC groups, which enhanced the comparability of the experimental results. Cognitive function assessment showed that the MMSE and MOCA scores of the AD group were significantly lower than those of the MCI group and the NC group, and the CDR scores were also significantly different, indicating that the cognitive functions of AD patients were severely impaired. As a pre-stage of AD, the MCI group had mild cognitive impairment, and early pathological changes such as Aβ deposition may have occurred in the brain. The trend of baseline cognitive function data scores in this study was consistent with previous studies.[27,28]

Exosomes are critical in the development of disease.[29] Serum exosomes are an ideal source of biomarkers and are widely available in serum, requiring only peripheral blood collection. This minimally invasive approach greatly reduces patient harm and improves the feasibility of sample collection and patient

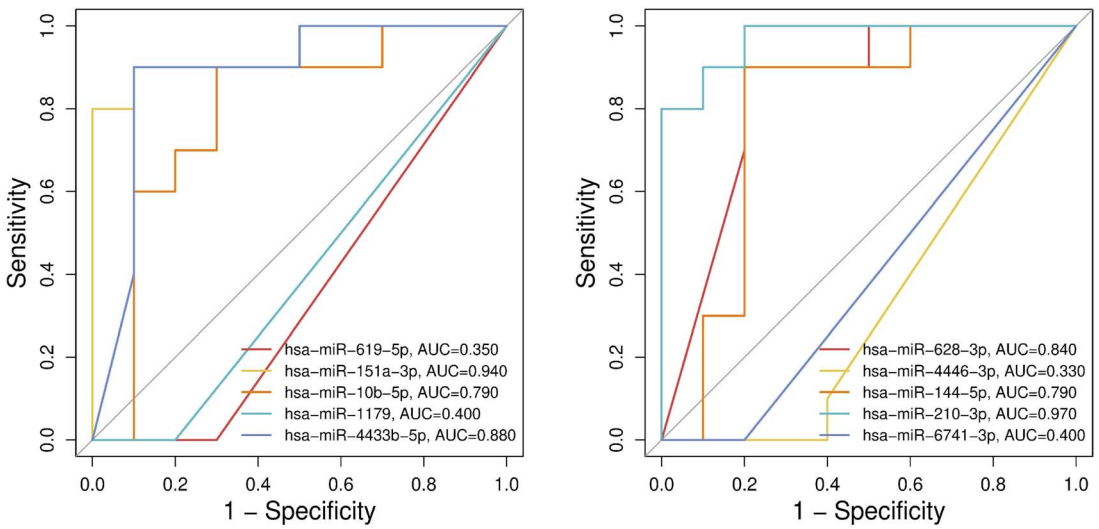

Fig. 5 The receiver operating characteristic (ROC) analysis of 10 common differentially expressed miRNAs in different comparison groups. Different color curves represent different miRNAs. AUC is the value of area under the curve, and greater than 0.05 indicates better performance.

compliance.[30] Compared to invasive ways of obtaining samples such as from cerebrospinal fluid, serum exosomes are easier and safer to collect.[31,32] Moreover, exosomes are rich in biomolecules, such as miRNAs, proteins, and DNA, which undergo specific changes during the development of AD and MCI. It was found that some miRNA expression profiles in serum exosomes of AD and MCI patients were significantly different from those of healthy people, which provided potential biomarkers for early diagnosis. In the field of drug discovery, the natural lipid bilayer structure of exosomes gives them good biocompatibility and stability, and enables them to effectively encapsulate various therapeutic drugs, such as small molecule drugs targeting AD and MCI, and deliver the drugs precisely to the lesion site to improve the drug efficacy and reduce the toxic side effects of the drugs on the normal tissues.[33,34]

In the present study, we successfully isolated the exosome from serum, and identified by TEM, NTA and nano-flow with reliable results. The exosomes showed a typical cup-shape and clear membrane structure under TEM, and NTA analysis showed that the particle size was in the common range, confirming that the extracted vesicles were exosomes. Then miRNA sequencing was performed on serum exosomes of three groups, and the miRNA expression profiles varied significantly from healthy to MCI to AD. GO and KEGG enrichment analysis of differentially expressed miRNA target genes revealed that biological processes and signaling pathways related to neural development, cellular communication, neurodegeneration and cellular senescence were involved in pairwise comparison. These suggested that exosomal miRNAs may affect cognitive decline during disease progression through the regulation of these key biological processes and signaling pathways.[35,36]

In our study, comparing the NC and MCI groups, 60 miRNAs were up-regulated and 386 miRNAs were down-regulated. In the MCI *versus* AD group, 254 miRNAs were upregulated and 70 miRNAs were downregulated. When NC was compared with the AD group, 64 miRNAs were up-regulated and 59 miRNAs were down-regulated. Notably, 10 common miRNAs were differentially expressed in the NC *versus* AD, MCI *versus* AD, and NC *versus* MCI comparisons. These miRNAs were likely to be involved in the core of disease development. AD and MCI have hidden symptoms in the early stage, and traditional diagnostic methods have certain limitations, which make it difficult to recognize the disease at an early stage.[37] These common miRNAs may be the first to undergo significant changes in expression levels when the disease is still in a subclinical state, *i.e.*, before the onset of obvious clinical symptoms.[38] Taking miR-210-3p and miR-151-3p as an example, their expression levels in the serum exosomes of AD and MCI patients are significantly different from those of healthy people, and show high sensitivity and specificity. By detecting these common differentially expressed miRNAs, the subtle changes in the early stage of the disease can be sharply captured and accurately distinguished from the healthy group, which is expected to break through the limitations of the traditional diagnostic methods and realize a more early, sensitive and specific diagnosis of the disease. These miRNAs further build a complex network of interactions with many mRNAs. Some miRNAs may interfere with the normal signaling pathways between nerve cells by inhibiting the expression of their corresponding mRNAs, which were often closely related to neural development, cellular communication, and neurodegeneration, *etc.*[39]

The study of these co-expressed miRNAs and their interaction networks can help us to localize the key signaling pathways and molecular nodes, and thus outline the molecular events of the disease from germination to progressive deterioration, which is crucial for the fundamental elucidation of the pathogenesis of AD and MCI.[40] Analysis of the interplay network revealed the presence of tightly linked miRNAs and mRNAs. Neuronal migration, differentiation, and synapse formation and plasticity are mediated by miRNA-mRNA regulatory networks in the developing nervous system.[41] Hippo signaling pathway regulates organ size, maintains tissue homeostasis and apoptosis balance, and is also involved in the regulation of neural stem cell proliferation and differentiation.[42] The axon guidance pathway directs axon extension guidance, which is essential for the construction of neural connectivity networks.[43] The regulation of neural pathways by these miRNAs provides new directions and targets for investigating the molecular mechanisms of neural development and the pathogenesis of related diseases. The results of ROC are important for evaluating the potential of miRNAs as biomarkers. The miR-151-3p, miR-10b-5p, miR-4433b-5p, miR-628-3p, miR-144-5p and miR-210-3p showed great potential as potential biomarkers for disease diagnosis or progression, with AUCs greater than 0.8, especially miR-210-3p and miR-151-3p. The AUC values of miR-10b-5p and miR-144-5p were close to 0.8, which did not reach the high diagnostic efficacy threshold but still showed moderate predictive ability. For miRNAs with lower AUC values, such as miR-619-5p, miR-1179, miR-4446-3p and miR-6741-3p, although the predictive ability of these miRNAs as biomarkers alone is limited, we can consider combining them with other indexes to explore their potential value in the comprehensive diagnostic system in the future.

Although some results have been obtained, future studies need to expand the sample size to enhance the generalizability and reliability of the findings. The establishment of animal models to simulate the disease process and *in vivo* validation of the key targets identified in this study are also important directions for future research. Finally, the longitudinal cohort studies can further confirm the change trajectory of exosomal miRNA from MCI to AD.

Conclusions

Overall, this study revealed the differences in cognitive functions and serum exosomal characteristics among the AD, MCI and healthy control groups through comprehensive comparisons. Serum exosomal miRNA expression profiles changed significantly from NC to MCI to AD, and 10 miRNAs were identified that may play key roles in the disease transition. The target gene and functional enrichment analyses further elucidated the mechanisms of cognitive decline through the regulation of neurodevelopment, cellular communication and other biological processes. Meanwhile, miRNAs with potential as

biomarkers for disease diagnosis or progression, such as miR-151-3p and miR-210-3p, were screened by ROC curve analysis. This study provides new insights into the pathogenesis of AD and MCI, and is expected to contribute to the improvement of early diagnosis and the development of therapeutic strategies for AD and MCI.

Ethics statement

The study was approved by the Ethics Committee of Chaning Mental Health Center, Shanghai, China (M202016), and complied with the Declaration of Helsinki. Written informed consent was obtained from all participants or their guardians.

Data availability

The data that support the findings of this study are available on request from the corresponding author. The data are not publicly available due to privacy or ethical restrictions.

Author contributions

Xi Chen, Silu Chen and Liangliang Chen designed and performed experiments, and prepared the figures. Hong Zheng and Jing Nie performed and analyzed experiments. Lingyan Yang contributed to the interpretation of the results and writing – review & editing. Xia Li and Kang Ju for the project administration and supervision. All authors have read and approved the final manuscript.

Conflicts of interest

The authors declare no conflict of interests.

Acknowledgements

The authors want to acknowledge the study participants for their dedication to the study. This study was supported by the Shanghai Municipal Health Commission project (202040500) and the National Key R&D Program of China (2023YFC3603200 and 2017YFC1310500).

References

1 R. Ren, J. Qi, S. Lin, X. Liu, P. Yin, Z. Wang, R. Tang, J. Wang, Q. Huang, J. Li, X. Xie, Y. Hu, S. Cui, Y. Zhu, X. Yu, P. Wang, Y. Zhu, Y. Wang, Y. Huang, Y. Hu, Y. Wang, C. Li, M. Zhou and G. Wang, *Gen. Psychiatry*, 2022, **35**, e100751.
2 C. Song, J. Shi, P. Zhang, Y. Zhang, J. Xu, L. Zhao, R. Zhang, H. Wang and H. Chen, *Transl. Neurodegener.*, 2022, **11**, 18.
3 J. A. Schneider, R. S. Wilson, J. L. Bienias, D. A. Evans and D. A. Bennett, *Neurology*, 2004, **62**, 1148–1155.
4 V. L. Villemagne, S. Burnham, P. Bourgeat, B. Brown, K. A. Ellis, O. Salvado, C. Szoeke, S. L. Macaulay, R. Martins, P. Maruff, D. Ames, C. C. Rowe, C. L. Masters and B. Australian, Imaging and G. Lifestyle Research, *Lancet Neurol.*, 2013, **12**, 357–367.
5 R. C. Petersen, *J. Intern. Med.*, 2004, **256**, 183–194.
6 B. Winblad, K. Palmer, M. Kivipelto, V. Jelic, L. Fratiglioni, L. O. Wahlund, A. Nordberg, L. Bäckman, M. Albert, O. Almkvist, H. Arai, H. Basun, K. Blennow, M. de Leon, C. DeCarli, T. Erkinjuntti, E. Giacobini, C. Graff, J. Hardy, C. Jack, A. Jorm, K. Ritchie, C. van Duijn, P. Visser and R. C. Petersen, *J. Intern. Med.*, 2004, **256**, 240–246.
7 P. Ding, X. Y. Ding, J. Y. Li, W. Guo, O. V. Okoro, M. Mirzaei, Y. F. Sun, G. H. Jiang, A. Shavandi and L. Nie, Facile preparation of self-healing hydrogels based on chitosan and PVA with the incorporation of curcumin-loaded micelles for wound dressings., *Biomed. Mater.*, 2023, **19**(2), 025021.
8 L. Yang, Y. Zhai, Y. Hao, Z. Zhu and G. Cheng, *Small*, 2020, **16**, e1906273.
9 M. Lu, W. Shao, H. Xing and Y. Huang, *Interdiscip. Med.*, 2023, **1**, e20220007.
10 L. R. Lizarraga-Valderrama and G. K. Sheridan, *FEBS Lett.*, 2021, **595**, 1391–1410.
11 K. Singh, R. Nalabotala, K. M. Koo, S. Bose, R. Nayak and M. J. A. Shiddiky, *Analyst*, 2021, **146**, 3731–3749.
12 Y. Zhai, Q. Wang, Z. Zhu, Y. Hao, F. Han, J. Hong, W. Zheng, S. Ma, L. Yang and G. Cheng, *Biomater. Sci.*, 2022, **10**, 5707–5718.
13 E. Eitan, T. Thornton-Wells, K. Elgart, E. Erden, E. Gershun, A. Levine, O. Volpert, M. Azadeh, D. G. Smith and D. Kapogiannis, *Extracell. Vesicles Circ. Nucleic Acids*, 2023, **4**, 133–150.
14 G.-Y. Xie, Y.-H. Deng, C.-J. Liu, A.-Y. Guo and Q. Lei, *Interdiscip. Med.*, 2025, **3**, e20240073.
15 I. Colvett, H. Saternos, C. Coughlan, A. Vielle and A. Ledreux, *Extracell. Vesicles Circ. Nucleic Acids*, 2023, **4**, 72–89.
16 Z. Dong, H. Gu, Q. Guo, S. Liang, J. Xue, F. Yao, X. Liu, F. Li, H. Liu, L. Sun and K. Zhao, Profiling of Serum Exosome MiRNA Reveals the Potential of a MiRNA Panel as Diagnostic Biomarker for Alzheimer's Disease, *Mol. Neurobiol.*, 2021, **58**, 3084–3094.
17 T. T. Yang, C. G. Liu, S. C. Gao, Y. Zhang and P. C. Wang, *Biomed. Environ. Sci.*, 2018, **31**, 87–96.
18 Z. Dong, H. Gu, Q. Guo, S. Liang, J. Xue, F. Yao, X. Liu, F. Li, H. Liu, L. Sun and K. Zhao, *Mol. Neurobiol.*, 2021, **58**, 3084–3094.
19 G. M. McKhann, D. S. Knopman, H. Chertkow, B. T. Hyman, C. R. Jack Jr, C. H. Kawas, W. E. Klunk, W. J. Koroshetz, J. J. Manly, R. Mayeux, R. C. Mohs, J. C. Morris, M. N. Rossor, P. Scheltens, M. C. Carrillo, B. Thies, S. Weintraub and C. H. Phelps, *Alzheimer's Dement.*, 2011, **7**, 263–269.
20 J. Lu, D. Li, F. Li, A. Zhou, F. Wang, X. Zuo, X. F. Jia, H. Song and J. Jia, *J. Geriatr. Psychiatr. Neurol.*, 2011, **24**, 184–190.
21 X. Jia, Z. Wang, F. Huang, C. Su, W. Du, H. Jiang, H. Wang, J. Wang, F. Wang, W. Su, H. Xiao, Y. Wang and B. Zhang, *BMC Psychiatry*, 2021, **21**, 485.
22 V. Dauphinot, S. Calvi, C. Moutet, J. Xie, S. Dautricourt, A. Batsavanis, P. Krolak-Salmon and A. Garnier-Crussard, *Alzheimers Res. Ther.*, 2024, **16**, 198.

23 L. M. Brown and J. A. Schinka, *Int. J. Geriatr. Psychiatr.*, 2005, **20**, 911–918.
24 S. Nagaraj, K. M. Zoltowska, K. Laskowska-Kaszub and U. Wojda, *Ageing Res. Rev.*, 2019, **49**, 125–143.
25 A. Baudry, S. Mouillet-Richard, B. Schneider, J. M. Launay and O. Kellermann, *Science*, 2010, **329**, 1537–1541.
26 J. Sanz-Ros, C. Mas-Bargues, N. Romero-García, J. Huete-Acevedo, M. Dromant and C. Borrás, *Extracell. Vesicles Circ. Nucleic Acids*, 2023, **4**, 486–501.
27 B. Frank, M. Walsh, L. Hurley, J. Groh, K. Blennow, H. Zetterberg, Y. Tripodis, A. E. Budson, M. K. O'Connor, B. Martin, J. Weller, A. McKee, W. Qiu, T. D. Stein, R. A. Stern, J. Mez, R. Henson, J. Long, A. J. Aschenbrenner, G. M. Babulal, J. C. Morris, S. Schindler and M. L. Alosco, *J. Alzheimers Dis.*, 2024, **100**, 1055–1073.
28 Y. Meng, H. Li, R. Hua, H. Wang, J. Lu, X. Yu and C. Zhang, *Sci. Rep.*, 2015, **5**, 15546.
29 Y. Huang, T. Arab, A. E. Russell, E. R. Mallick, R. Nagaraj, E. Gizzie, J. Redding-Ochoa, J. C. Troncoso, O. Pletnikova, A. Turchinovich, D. A. Routenberg and K. W. Witwer, *Interdiscip. Med.*, 2023, **1**, e20230016.
30 W. Zou, M. Lai, Y. Jiang, L. Mao, W. Zhou, S. Zhang, P. Lai, B. Guo, T. Wei, C. Nie, L. Zheng, J. Zhang, X. Gao, X. Zhao, L. Xia, Z. Zou, A. Liu, S. Liu, Z. K. Cui and X. Bai, *Adv. Sci.*, 2023, **10**, e2204826.
31 A. M. Eteleeb, B. C. Novotny, C. S. Tarraga, C. Sohn, E. Dhungel, L. Brase, A. Nallapu, J. Buss, F. Farias, K. Bergmann, J. Bradley, J. Norton, J. Gentsch, F. Wang, A. A. Davis, J. C. Morris, C. M. Karch, R. J. Perrin, B. A. Benitez and O. Harari, *PLoS Biol.*, 2024, **22**, e3002607.
32 K. Boriachek, M. N. Islam, A. Möller, C. Salomon, N. T. Nguyen, M. S. A. Hossain, Y. Yamauchi and M. J. A. Shiddiky, *Small*, 2018, **14**(6), 1–21.
33 H. Xie, J. Yao, Y. Wang and B. Ni, *Drug Delivery*, 2022, **29**, 1257–1271.
34 H. A. Dad, T. W. Gu, A. Q. Zhu, L. Q. Huang and L. H. Peng, *Mol. Ther.*, 2021, **29**, 13–31.
35 P. Zou, C. Wu, T. C. Liu, R. Duan and L. Yang, *Transl. Neurodegener.*, 2023, **12**, 52.
36 I. G. Onyango, G. V. Jauregui, M. Carna, J. P. Bennett Jr and G. B. Stokin, *Biomedicines*, 2021, **9**(2), 524–534.
37 Y. Chen, M. Al-Nusaif, S. Li, X. Tan, H. Yang, H. Cai and W. Le, *Front. Med.*, 2024, **18**, 446–464.
38 J. Graff-Radford, K. X. X. Yong, L. G. Apostolova, F. H. Bouwman, M. Carrillo, B. C. Dickerson, G. D. Rabinovici, J. M. Schott, D. T. Jones and M. E. Murray, *Lancet Neurol.*, 2021, **20**, 222–234.
39 L. D. Nguyen, Z. Wei, M. C. Silva, S. Barberan-Soler, J. Zhang, R. Rabinovsky, C. R. Muratore, J. M. S. Stricker, C. Hortman, T. L. Young-Pearse, S. J. Haggarty and A. M. Krichevsky, *Nat. Commun.*, 2023, **14**, 7575.
40 A. Muniategui, J. Pey, F. J. Planes and A. Rubio, *Briefings Bioinf.*, 2013, **14**, 263–278.
41 T. Kazemi, S. Huang, N. G. Avci, C. M. K. Waits, Y. M. Akay and M. Akay, *Sci. Rep.*, 2020, **10**, 15016.
42 J. Gil-Ranedo, E. Gonzaga, K. J. Jaworek, C. Berger, T. Bossing and C. S. Barros, *Cell Rep.*, 2019, **27**, 2921–2933.
43 S. J. Kim, W. K. Ko, G. H. Han, D. Lee, M. J. Cho, S. H. Sheen and S. Sohn, *Biomater. Res.*, 2023, **27**, 101.